Measurements and interpretations of Simplified Template Cross Sections, differential and fiducial cross sections in Higgs boson decays to four leptons with the ATLAS detector

Samyukta Krishnamurthy

On behalf of the ATLAS collaboration

University of Massachusetts, Amherst

ATLAS EXPERIMENT

Higgs 2021

Thursday, October 21st

UMassAmherst

ATLAS EXPERIMENT

UMassAmherst

Introduction

- Talk summarizes recent ATLAS results specifically in the $H \rightarrow 4\ell$ decay channel
  - Fiducial and differential cross-section measurements
    - Eur. Phys. J. C 80 (2020) 942
  - Simplified Template Cross Section measurements (STXS) and EFT interpretation
    - Eur. Phys. J. C 80 (2020) 957

- Overview : $H \rightarrow \mathbf{4\ell}$ Channel

  Clean experimental signature – fully reconstructed final states
    - Full access to Higgs kinematics
    - High (2:1) Signal to Background ratio => precision measurements

$H \to 4\ell$ fiducial and differential cross section – Analysis overview

Event selection (Detailed S:17)

Same-flavor opposite sign lepton pairs form Higgs candidates.

Background Estimation

Data driven techniques used to constrain normalization for the dominant non-resonant ZZ* background.

Other reducible background processes, such as Z+jets, $t\bar{t}$, and WZ are significantly smaller than the ZZ^* background and are estimated using data where possible.

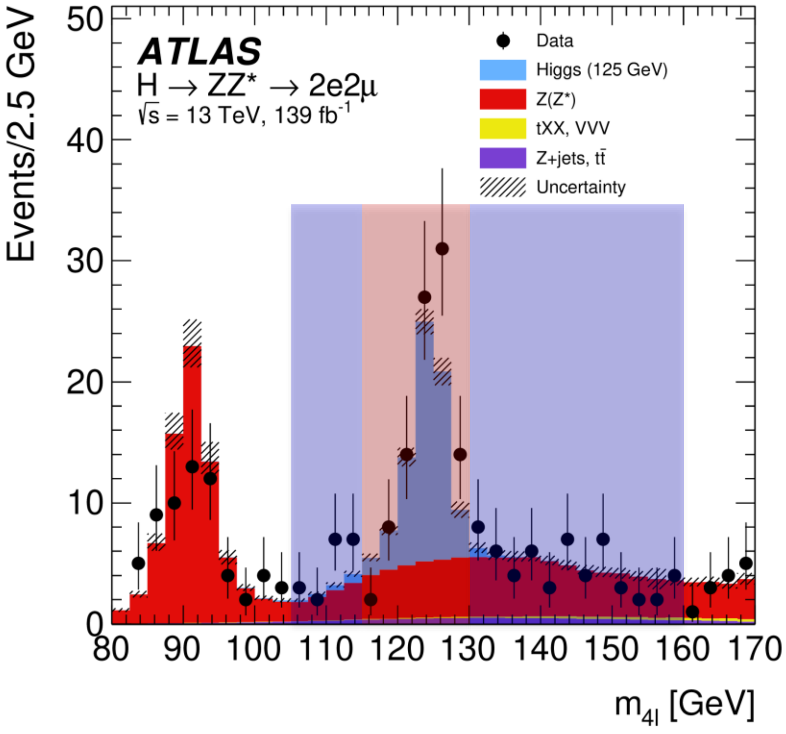

$H \rightarrow 4\ell$ fiducial cross section – Results

Fiducial region defined as close as possible to event selection to minimize extrapolation. Acceptance efficiency ~50%

Signal events extraction

For each decay state, the invariant mass template for the signal and background are fitted to the data $m_{4\ell}$.

$\sigma_{comb,fid}$: 3.28 ± 0.30 ± 0.11 [fb]
$\sigma_{SM,fid}$: 3.41 ± 0.18 [fb]

$\sigma_{tot,}$: 53.5 ± 4.9 ± 2.1 [pb]
$\sigma_{SM,tot}$: 55.7 ± 2.8 [pb]

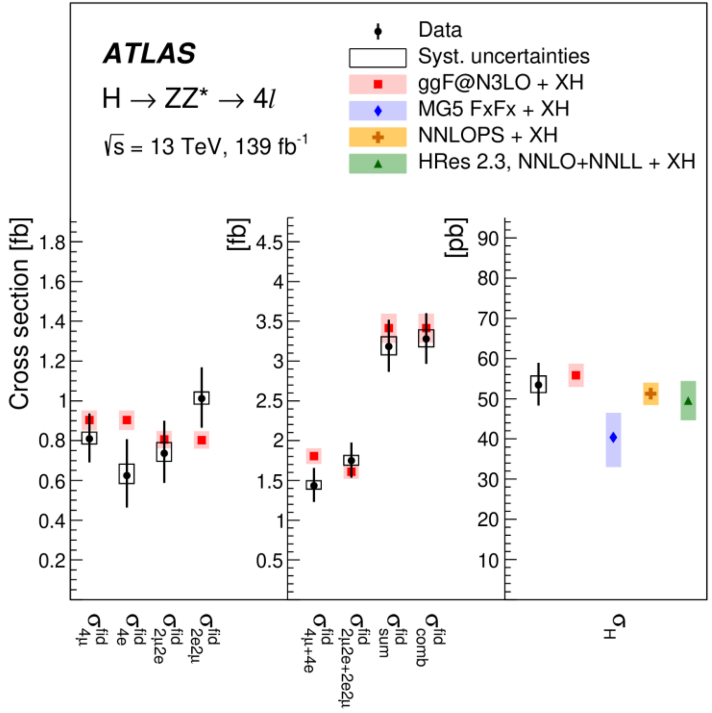

$H \rightarrow 4\ell$ differential cross section – Overview

Samyukta Krishnamurthy

Observables:

Differential cross sections are measured for several variables that are sensitive to Higgs production and decay (Full list S:18)

For each bin, the invariant mass template for the signal and background are fitted to the data $m_{4\ell}$

Efficiency and event migrations are corrected via response matrix obtained from simulation.

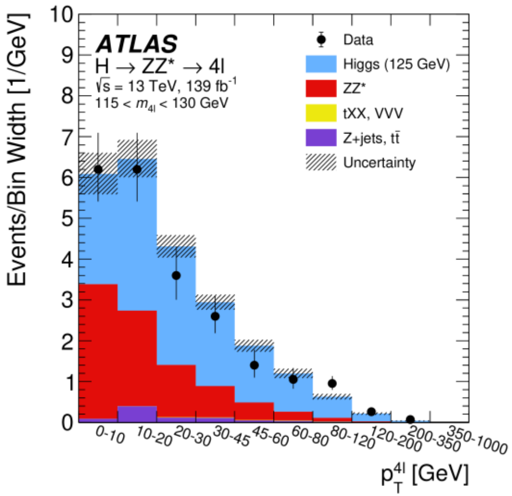

The observed and expected (pre-fit) distributions for $p_T^{4\ell}$

Response matrices, derived using simulation, for $p_T^{4\ell}$

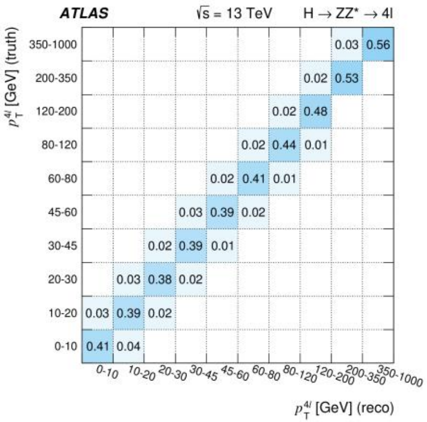

Higgs 2021

$H \rightarrow 4\ell$ differential cross section – Overview

Observables:

Differential cross sections are measured for several variables that are sensitive to Higgs production and decay (Full list S:20)

Representative examples:

$p_{\mathrm{T}}^{4\ell}$ – Higgs Transverse momentum sensitive to :

- higher order QCD corrections to Higgs boson production
- charm and bottom Yukawa couplings.

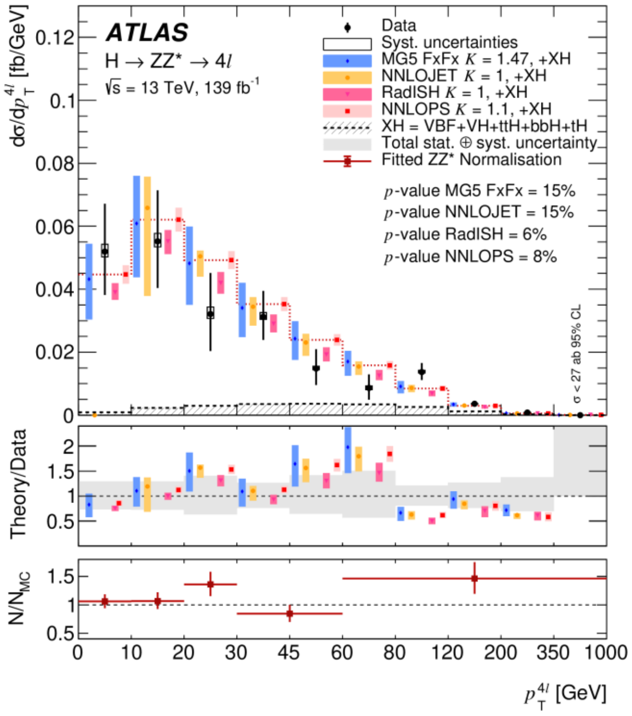

$H \to 4\ell$ differential cross section – Overview

Observables:

Differential cross sections are measured for several variables that are sensitive to Higgs production and decay (Full list S:20)

Representative examples:

m_{12}, m_{34} – Invariant mass of the leading (SFOS lepton pair with mass closest to the Z boson mass) and subleading lepton (the other pair) pair :

- sensitive to higher-order electroweak corrections to the Higgs boson decay
- BSM contributions

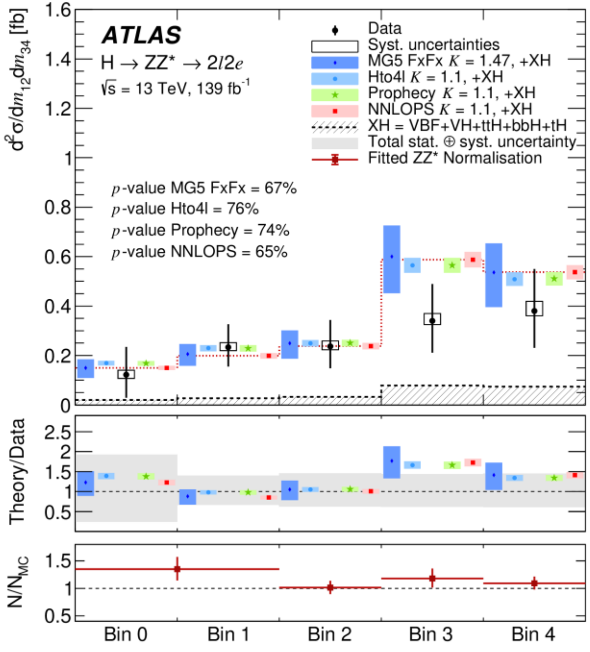

m_{12} vs. m_{34}

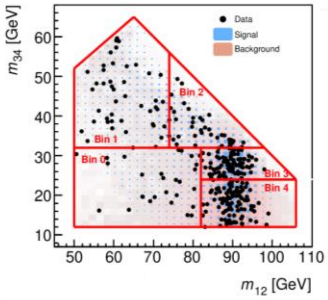

$H \to 4\ell$ differential cross section – Overview

Observables:

Differential cross sections are measured for several variables that are … production and decay (F…

Representative exam…

m_{12}, m_{34} – Invariant ma… (SFOS lepton pair with m… boson mass) and subleading lepton (the other pair) pair :

- sensitive to higher-order electroweak corrections to the Higgs boson decay
- BSM contributions

Good agreement between measured cross sections and predictions

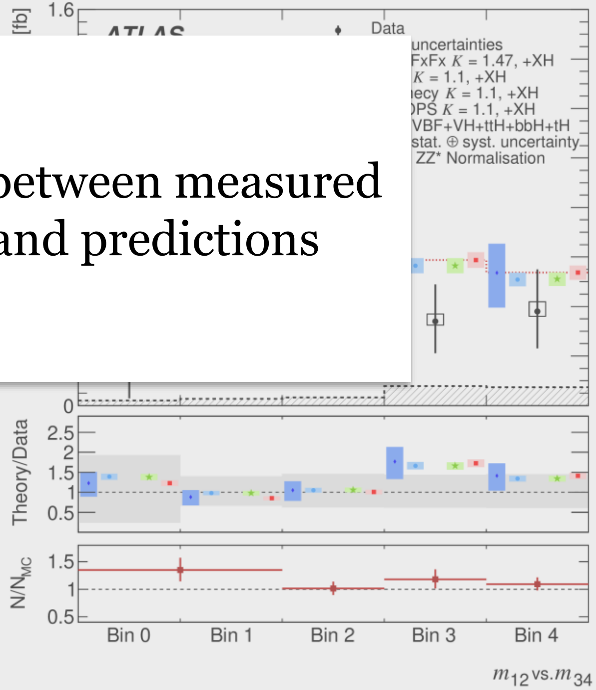

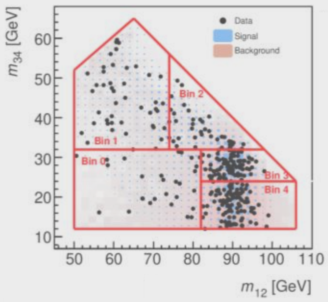

$H \rightarrow 4\ell$ fiducial and differential cross section – Interpretation

Analysis of the $p_T^{4\ell}$ spectrum allows for indirect constraints on the Yukawa coupling of the Higgs boson to charm (κ_c) and bottom quarks (κ_b).

Three cases considered, with increasing level of model dependency, to constrain κ_c and κ_b.

- Only the $p_T{}^{4\ell}$ shape is used
- the predicted $p_T{}^{4\ell}$ differential cross section is used
- both the prediction of the $p_T{}^{4\ell}$ differential cros section and the modification to the branching ratio are used

Interpretation	Parameter best-fit value	95% confidence interval
Modifications to only $p_T^{4\ell}$ shape	$\kappa_c = -1.1$	$[-11.7, 10.5]$
	$\kappa_b = 0.28$	$[-3.21, 4.50]$
Modifications to $p_T^{4\ell}$ predictions	$\kappa_c = 0.66$	$[-7.46, 9.27]$
	$\kappa_b = 0.55$	$[-1.82, 3.34]$

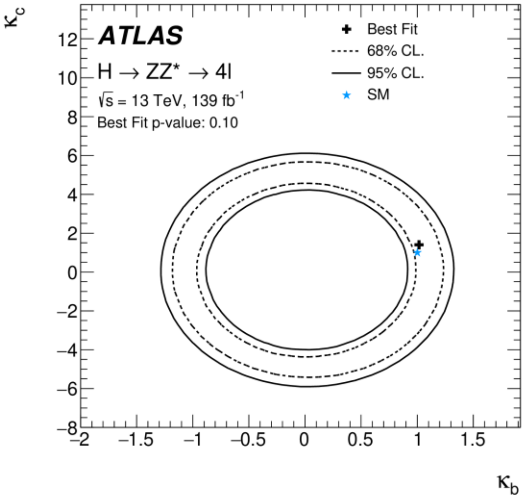

Observed direct constraint on the charm Yukawa coupling modifier $|\kappa_c|< 8.5$ [ATLAS-CONF-2021-021]

$H \rightarrow 4\ell$ STXS – Overview

ATLAS EXPERIMENT

UMassAmherst

STXS reduced Stage-1.1 framework is used to measure the Higgs boson production cross-sections.

Production bins are defined based on several kinematic variables like $p_T^{4\ell}$, number of jets, number of b-jets, m_{jj} etc.

The normalization for the dominant background in each bin is constrained using jet-multiplicity based sideband categories.

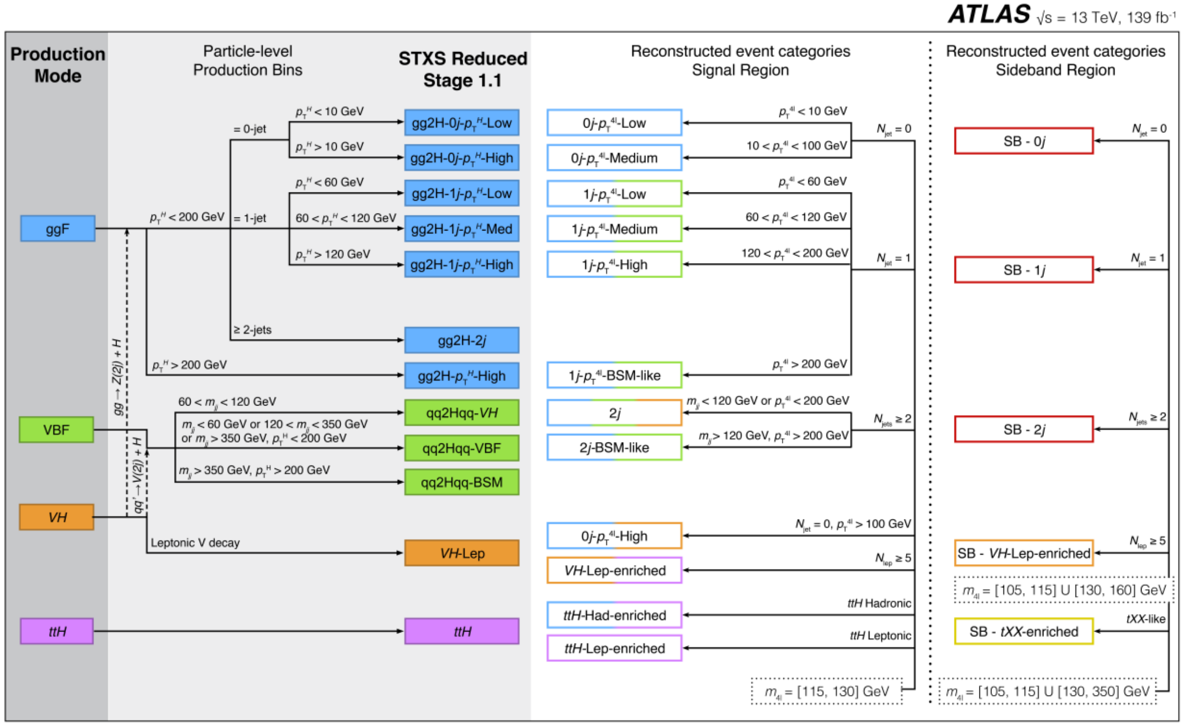

$H \rightarrow 4\ell$ STXS – Overview

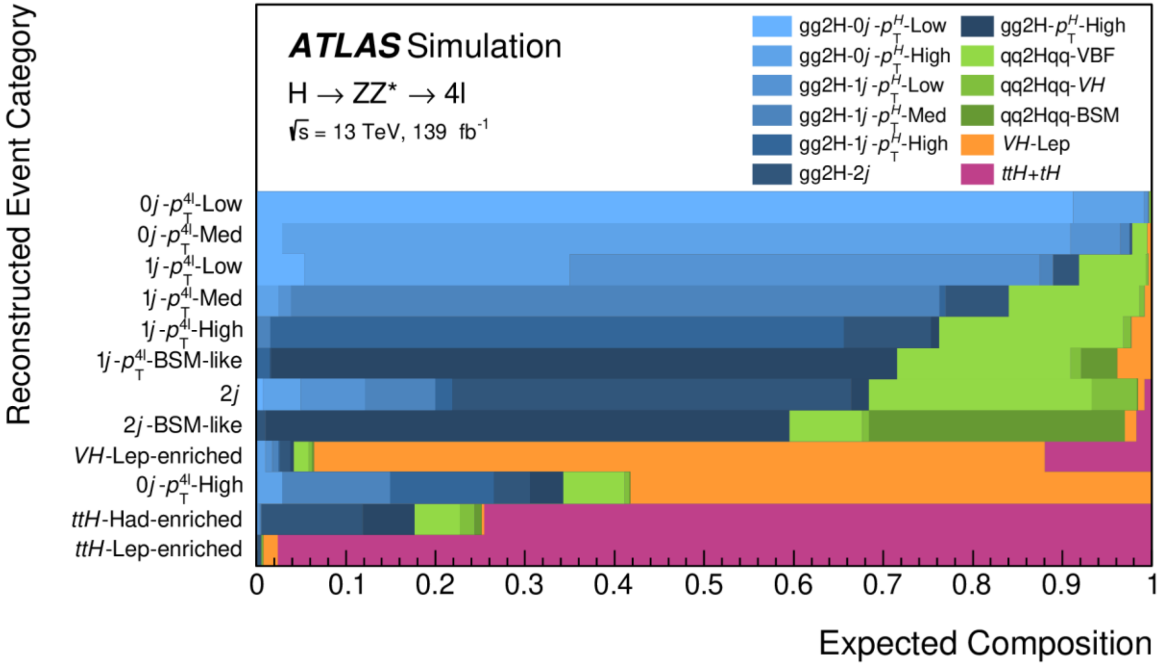

Neural networks (both MLPs and RNNs) are used within production bins to further isolate different production modes and the backgrounds.

Depending on the category and the number of classes (processes of interest), the NN has two or three outputs corresponding to the probability of belonging to each class.

$H \rightarrow 4\ell$ STXS – Results

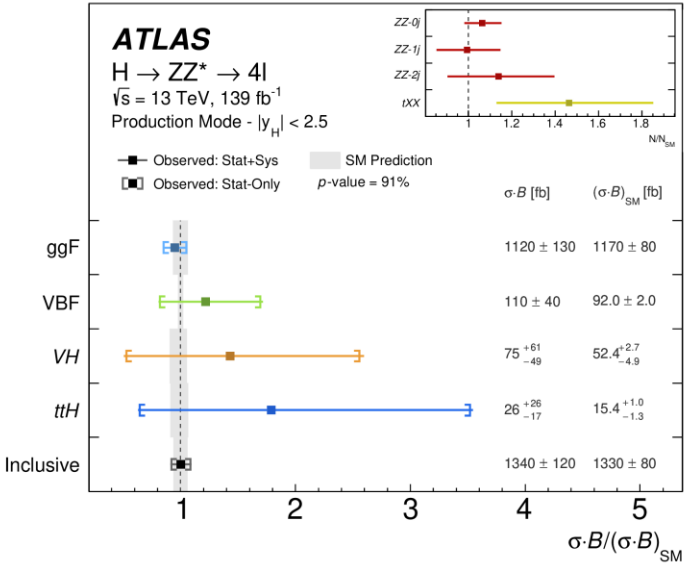

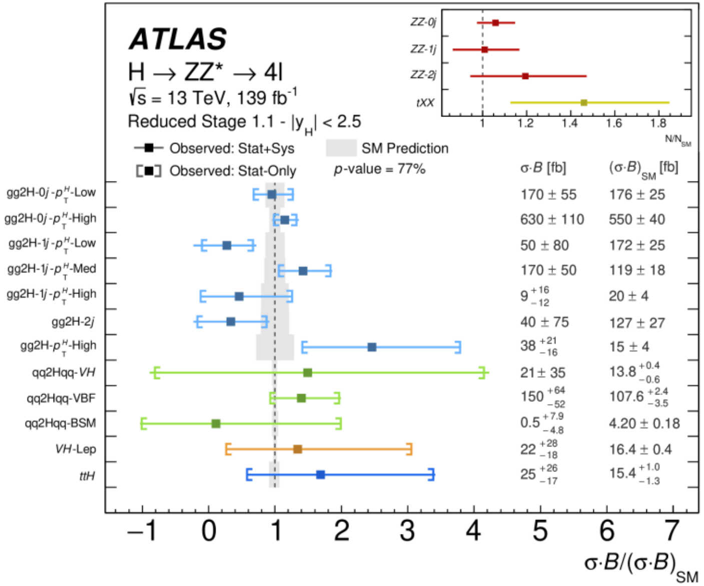

The observed and expected SM values of the cross-sections normalized by the SM expectation in the Production Mode Stage (Left) and the Reduced Stage-1.1 production bins (Right)

$H \to 4\ell$ STXS – EFT interpretation

STXS results are used to constrain the possible contributions from BSM physics to the relevant vertices within the Standard Model Effective Field Theory (SMEFT) formalism

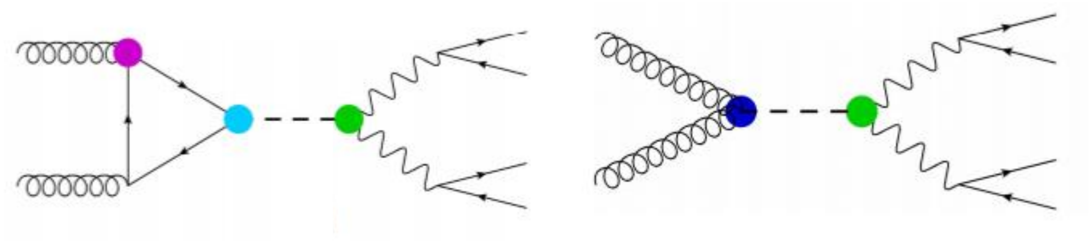

Several dimension-6 EFT operators probed.

CP-even Operator	CP-even Structure	CP-even Coeff.	CP-odd Operator	CP-odd Structure	CP-odd Coeff.	Impact on production	Impact on decay
O_{uH}	$HH^\dagger \bar{q}_p u_r \tilde{H}$	c_{uH}	O_{uH}	$HH^\dagger \bar{q}_p u_r \tilde{H}$	$c_{\tilde{u}H}$	ttH	-
O_{HG}	$HH^\dagger G^A_{\mu\nu} G^{\mu\nu A}$	c_{HG}	$O_{H\tilde{G}}$	$HH^\dagger \tilde{G}^A_{\mu\nu} G^{\mu\nu A}$	$c_{H\tilde{G}}$	ggF	Yes
O_{HW}	$HH^\dagger W^l_{\mu\nu} W^{\mu\nu l}$	c_{HW}	$O_{H\tilde{W}}$	$HH^\dagger \tilde{W}^l_{\mu\nu} W^{\mu\nu l}$	$c_{H\tilde{W}}$	VBF, VH	Yes
O_{HB}	$HH^\dagger B_{\mu\nu} B^{\mu\nu}$	c_{HB}	$O_{H\tilde{B}}$	$HH^\dagger \tilde{B}_{\mu\nu} B^{\mu\nu}$	$c_{H\tilde{B}}$	VBF, VH	Yes
O_{HWB}	$HH^\dagger \tau^l W^l_{\mu\nu} B^{\mu\nu}$	c_{HWB}	$O_{H\tilde{W}B}$	$HH^\dagger \tau^l \tilde{W}^l_{\mu\nu} B^{\mu\nu}$	$c_{H\tilde{W}B}$	VBF, VH	Yes

$H \rightarrow 4\ell$ STXS – EFT interpretation

EFT signal model is built by parameterizing the production cross-sections (per production bin), the branching ratio and the signal acceptances, as a function of the SMEFT Wilson coefficients

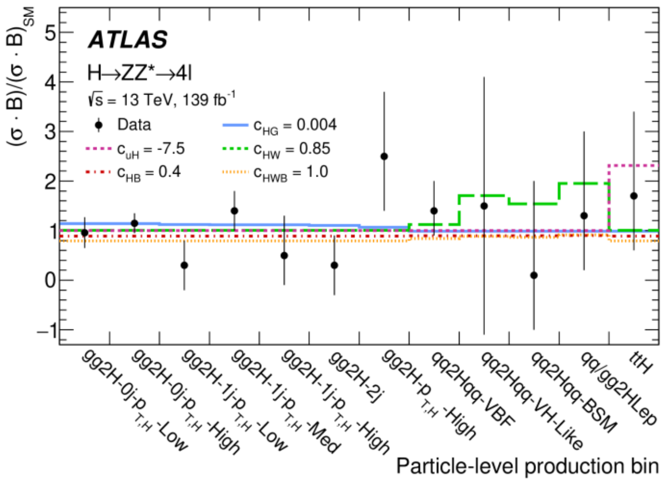

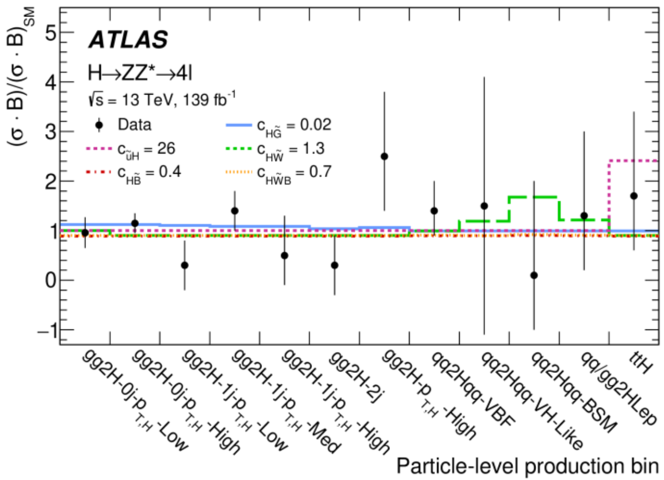

The expected signal yield ratio for CP-even (Left) and CP-odd (Right) EFT parameter values together with the corresponding cross-section measurement in each production bin

$H \rightarrow 4\ell$ STXS – EFT interpretation

The fit results with only one Wilson coefficient fitted at a time. Measurements are dominated by statistical uncertainty and measured values of all the coefficients are consistent with 0.

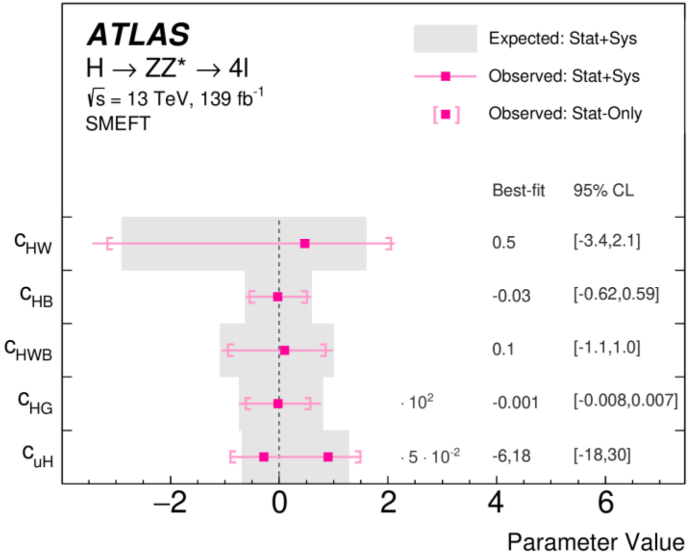

CP - Even

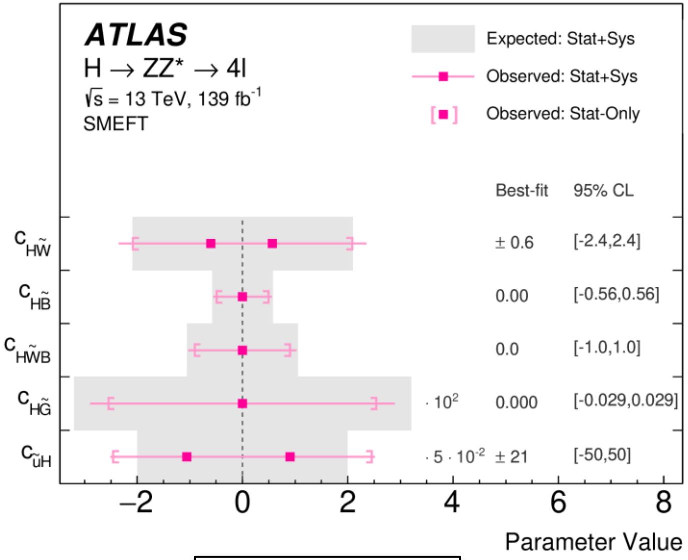

CP - Odd

Conclusions

- Summarized most recent ATLAS measurements on Higgs cross-section in the **4ℓ** channel
  - STXS, fiducial, and differential XS results summarized
  - Full run- II data (139^{-1} fb) taken into consideration
  - All measurements consistent with the Standard Model
- Many interesting results thanks to
  - $H \rightarrow$ **4ℓ** channel's clean signature
  - Run II data => less statistical limitations
- Looking forward to updated results with Run-III!

BACKUP

$H \rightarrow 4\ell$ fiducial and differential cross section

Event selection

Same-flavor opposite sign lepton pairs form Higgs candidates

Leptons and jets	
Leptons	$p_T > 5$ GeV, $\lvert\eta\rvert < 2.7$
Jets	$p_T > 30$ GeV, $\lvert y\rvert < 4.4$
Lepton selection and pairing	
Lepton kinematics	$p_T > 20, 15, 10$ GeV
Leading pair (m_{12})	SFOC lepton pair with smallest $\lvert m_Z - m_{\ell\ell}\rvert$
Subleading pair (m_{34})	remaining SFOC lepton pair with smallest $\lvert m_Z - m_{\ell\ell}\rvert$
Event selection (at most one quadruplet per event)	
Mass requirements	50 GeV$< m_{12} <$ 106 GeV and 12 GeV $< m_{34} <$ 115 GeV
Lepton separation	$\Delta R(\ell_i, \ell_j) > 0.1$
Lepton/Jet separation	$\Delta R(\ell_i, \text{jet}) > 0.1$
J/ψ veto	$m(\ell_i, \ell_j) > 5$ GeV for all SFOC lepton pairs
Mass window	105 GeV $< m_{4\ell} <$ 160 GeV
If extra lepton with $p_T > 12$ GeV	Quadruplet with largest matrix element value

Fiducial region defined as close as possible to event selection to minimize extrapolation. Acceptance efficiency ~50%

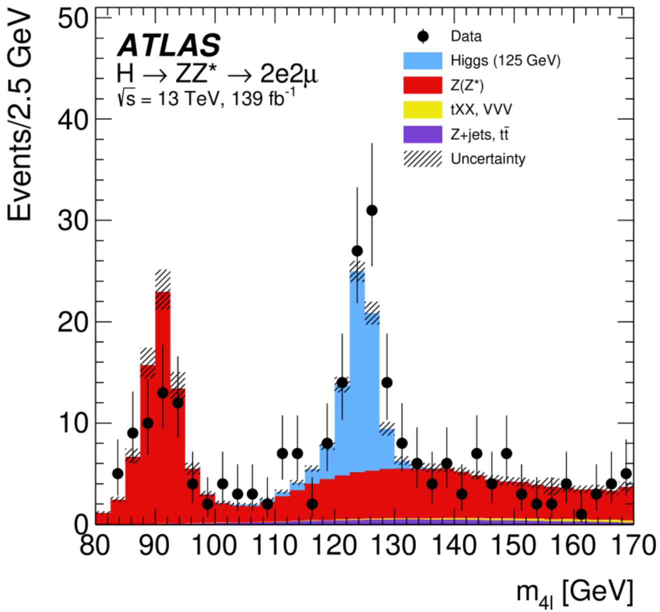

ZZ* Background Estimation

Data driven techniques used to constrain normalization for the dominant background.

$H \rightarrow 4\ell$ differential cross section

ATLAS EXPERIMENT

UMassAmherst

Higgs boson kinematic-related variables	
$p_{\mathrm{T}}^{4\ell}$, $\lvert y_{4\ell} \rvert$	Transverse momentum and rapidity of the four-lepton system
m_{12}, m_{34}	Invariant mass of the leading and subleading lepton pair
$\lvert \cos\theta^* \rvert$	Magnitude of the cosine of the decay angle of the leading lepton pair in the four-lepton rest frame relative to the beam axis
$\cos\theta_1$, $\cos\theta_2$	Production angles of the anti-leptons from the two Z bosons, where the angle is relative to the Z vector.
ϕ, ϕ_1	Two azimuthal angles between the three planes constructed from the Z bosons and leptons in the Higgs boson rest frame.
Jet-related variables	
N_{jets}, $N_{b\text{-jets}}$	Jet and b-jet multiplicity
$p_{\mathrm{T}}^{\mathrm{lead.\ jet}}$, $p_{\mathrm{T}}^{\mathrm{sublead.\ jet}}$	Transverse momentum of the leading and subleading jet, for events with at least one and two jets, respectively. Here, the leading jet refers to the jet with the highest p_{T} in the event, while subleading refers to the jet with the second-highest p_{T}.
m_{jj}, $\lvert\Delta\eta_{jj}\rvert$, $\Delta\phi_{jj}$	Invariant mass, difference in pseudorapidity, and signed difference in ϕ of the leading and subleading jets for events with at least two jets
Higgs boson and jet-related variables	
$p_{\mathrm{T}}^{4\ell\mathrm{j}}$, $m_{4\ell j}$	Transverse momentum and invariant mass of the four-lepton system and leading jet, for events with at least one jet
$p_{\mathrm{T}}^{4\ell\mathrm{jj}}$, $m_{4\ell jj}$	Transverse momentum and invariant mass of the four-lepton system and leading and subleading jets, for events with at least two jets

$H \to ZZ$ pseudo-observables interpretation

- The measured differential fiducial cross sections can be used to probe possible effects of physics beyond the SM.
- The $m_{12} \times m_{34}$ differential cross section is used to interpret the measurement as a function of pseudo-observables.
- The $p_T^{4\ell}$ differential cross section is used to constrain the Yukawa couplings of the Higgs boson to b and c-quarks.

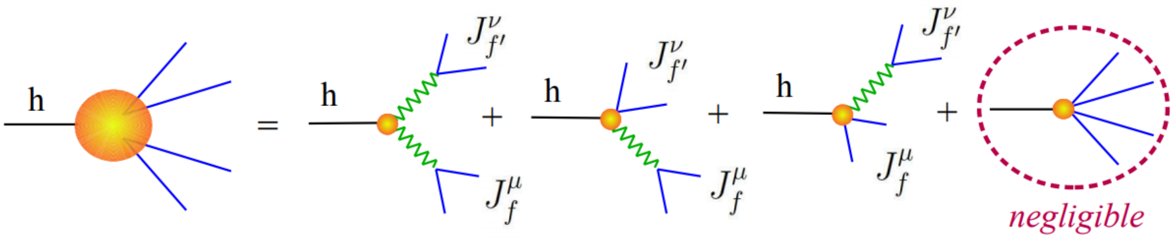

$$\begin{aligned}
\mathcal{A} =& i\frac{2m_Z^2}{v_F}\sum_{e=e_L,e_R}\sum_{\mu=\mu_L,\mu_R}(\bar{e}\gamma_\alpha e)(\bar{\mu}\gamma_\beta\mu)\times \\
&\Bigg[\left(\kappa_{ZZ}\frac{g_Z^e g_Z^\mu}{P_Z(q_1^2)P_Z(q_2^2)}+\frac{\epsilon_{Ze}}{m_Z^2}\frac{g_Z^\mu}{P_Z(q_2^2)}+\frac{\epsilon_{Z\mu}}{m_Z^2}\frac{g_Z^e}{P_Z(q_1^2)}\right)g^{\alpha\beta}+ \\
&+\left(\epsilon_{ZZ}\frac{g_Z^e g_Z^\mu}{P_Z(q_1^2)P_Z(q_2^2)}+\kappa_{Z\gamma}\epsilon_{Z\gamma}^{\text{SM-1L}}\left(\frac{eQ_\mu g_Z^e}{q_2^2 P_Z(q_1^2)}+\frac{eQ_e g_Z^\mu}{q_1^2 P_Z(q_2^2)}\right)+\kappa_{\gamma\gamma}\epsilon_{\gamma\gamma}^{\text{SM-1L}}\frac{e^2 Q_e Q_\mu}{q_1^2 q_2^2}\right)\frac{q_1\cdot q_2\, g^{\alpha\beta}-q_2{}^\alpha q_1{}^\beta}{m_Z^2}+ \\
&+\left(\epsilon_{ZZ}^{\text{CP}}\frac{g_Z^e g_Z^\mu}{P_Z(q_1^2)P_Z(q_2^2)}+\epsilon_{Z\gamma}^{\text{CP}}\left(\frac{eQ_\mu g_Z^e}{q_2^2 P_Z(q_1^2)}+\frac{eQ_e g_Z^\mu}{q_1^2 P_Z(q_2^2)}\right)+\epsilon_{\gamma\gamma}^{\text{CP}}\frac{e^2 Q_e Q_\mu}{q_1^2 q_2^2}\right)\frac{\varepsilon^{\alpha\beta\rho\sigma}q_{2\rho}q_{1\sigma}}{m_Z^2}\Bigg]
\end{aligned}$$

$$\epsilon_{\gamma\gamma}^{\text{SM-1L}} \simeq 3.8\times10^{-3}$$
$$\epsilon_{Z\gamma}^{\text{SM-1L}} \simeq 6.7\times10^{-3}$$

$$P_Z(q^2) = q^2 - m_Z^2 + i m_Z \Gamma_Z$$

$H \to ZZ$ pseudo-observables interpretation

- The measured differential fiducial cross sections can be used to probe possible effects of physics beyond the SM.
- The $m_{12} \times m_{34}$ differential cross section is used to interpret the measurement as a function of pseudo-observables.
- The $p_T^{4\ell}$ differential cross section is used to constrain the Yukawa couplings of the Higgs boson to b and c-quarks.

flavor-universal contact terms

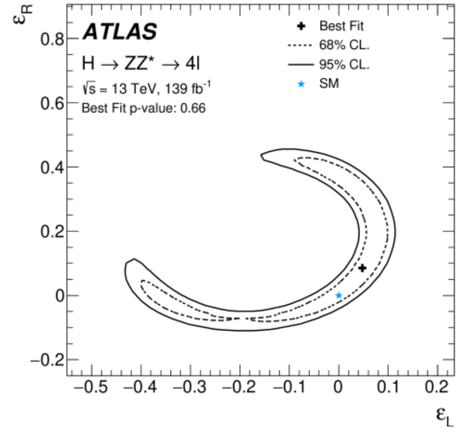

linear EFT inspired

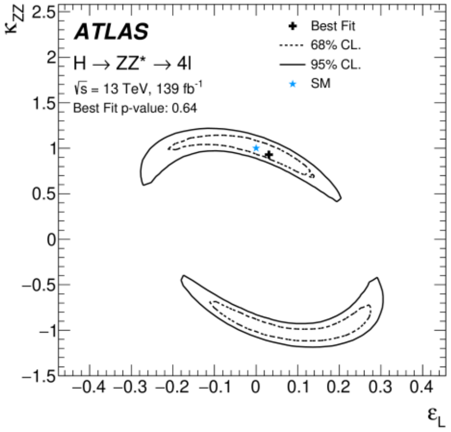

flavor non-universal vector contact terms

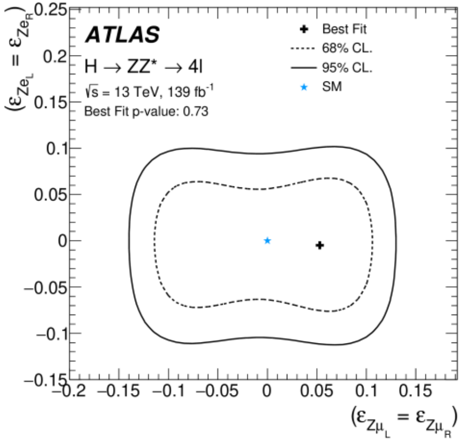

flavor non-universal axial contact terms

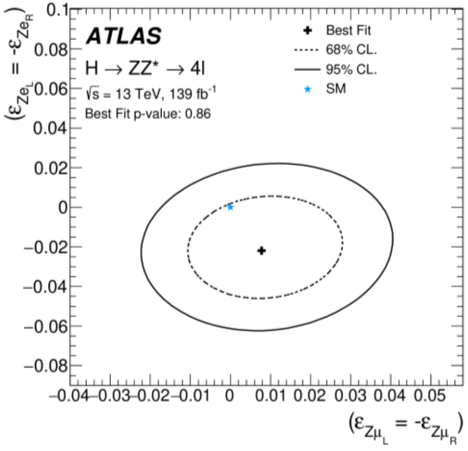

Samyukta Krishnamurthy

$H \to 4\ell$ fiducial and differential cross section – interpretation

UMassAmherst

Analysis of the $p_T^{4\ell}$ spectrum allows for indirect constrains on the Yukawa coupling of the Higgs boson to specifically, to charm (κ_c) and bottom quarks (κ_b).

Three cases considered, with increasing level of model dependency, to constrain κ_c and κ_b.

- Only the $p_T{}^{4\ell}$ shape is used

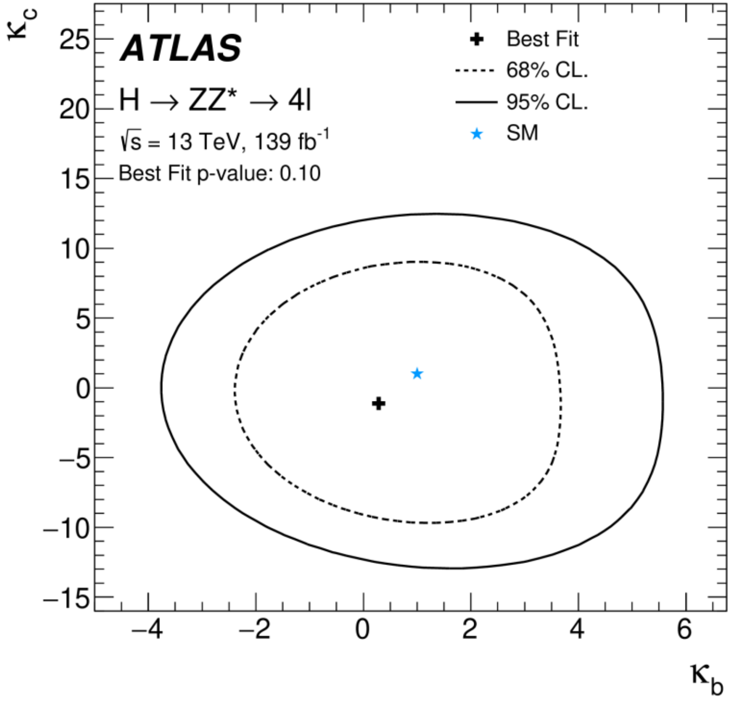

$H \rightarrow 4\ell$ fiducial and differential cross section – interpretation

Analysis of the $p_T^{4\ell}$ spectrum allows for indirect constrains on the Yukawa coupling of the Higgs boson to specifically, to charm (κ_c) and bottom quarks (κ_b).

Three cases considered, with increasing level of model dependency, to constrain κ_c and κ_b.

- Only the $p_T^{4\ell}$ shape is used
- the predicted $p_T^{4\ell}$ differential cross section is used

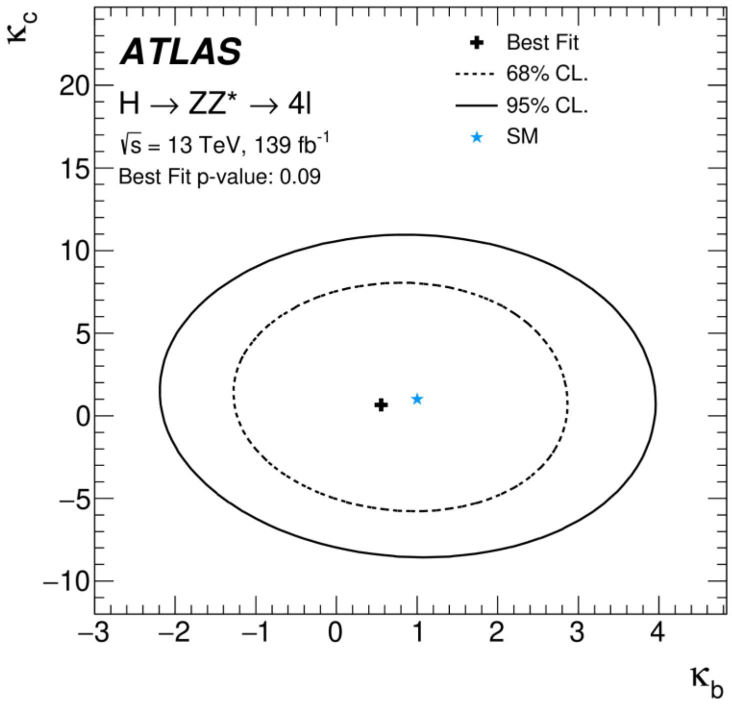

UMassAmherst

The Commonwealth's Flagship Campus